Shock and Vibration 20 (2013) 847–861
DOI 10.3233/SAV-130789
IOS Press

Mid frequency shock response determination by using energy flow method and time domain correction

Sung-Hyun Woo[a] and Jae-Hung Han[b,*]
[a]*KOMPSAT-5 System Engineering and Integration Team, Korea Aerospace Research Institute, Daejeon, Korea*
[b]*Department of Aerospace Engineering, Korea Advanced Institute of Science and Technology, Daejeon, Korea*

Received 28 October 2012
Revised 11 March 2013
Accepted 14 March 2013

Abstract. Shock induced vibration can be more crucial in the mid frequency range where the dynamic couplings with structural parts and components play important roles. To estimate the behavior of structures in this frequency range where conventional analytical schemes, such as statistical energy analysis (SEA) and finite element analysis (FEA) methods may become inaccurate, many alternative methodologies have been tried up to date. This study presents an effective and practical method to accurately predict transient responses in the mid frequency range without having to resort to the large computational efforts. Specifically, the present study employs the more realistic frequency response functions (FRFs) from the energy flow method (EFM) which is a hybrid method combining the pseudo SEA equation (or SEA-Like equation) and modal information obtained by the finite element analysis (FEA). Furthermore, to obtain the time responses synthesized with modal characteristics, a time domain correction is practiced with the input force signal and the reference FRF on a position of the response subsystem. A numerical simulation is performed for a simple five plate model to show its suitability and effectiveness over the standard analytical schemes.

Keywords: Vibro-acoustic, mid frequency, shock response, finite element analysis (FEA), shock response spectrum (SRS), statistical energy analysis (SEA), energy flow method (EFM), virtual modal synthesis and simulation (VMSS), time domain correction

1. Introduction

Pyrotechnical shock devices are broadly used in the aerospace engineering field, especially for satellite separation and appendage deployment mechanisms, and thus the activation of those devices often induces high-level dynamic structural responses due to the transient release of their strain energy. This high-acceleration, high frequency pyroshock can induce malfunction of electrical components of a launch vehicle or a satellite, resulting in a catastrophic mission failure [1]. Therefore prediction of the shock induced responses of structures is an essential work when pyro devices are employed [2]. For this practical purpose, an empirical method based on the measurement data of heritage programs used to be applied just to obtain an approximated level of shock that would be induced in structural parts of interest [3,4]. When a statistical energy analysis (SEA) model is available for acoustic and high frequency vibration problems, it can be used to provide band-averaged frequency response functions (FRFs) for virtual mode synthesis and simulation (VMSS) [5,6]. However, considering the fact that the structural behavior in the mid frequency range is often critical due to local resonances of the structure and dynamic couplings induced by

*Corresponding author: Jae-Hung Han, Department of Aerospace Engineering, Korea Advanced Institute of Science and Technology, Daejeon 305-701, Korea. Tel.: +82 42 350 3723; Fax: +82 42 350 3710; E-mail: jaehunghan@kaist.ac.kr.

ISSN 1070-9622/13/$27.50 © 2013 – IOS Press and the authors. All rights reserved

them, the SEA approach which was originally developed for high frequency vibroacoustic problems may become inappropriate for application to the mid frequency range.

In order to overcome the inherent limitation of SEA in the mid frequency range, hybrid FEM/SEA approaches have been investigated; several cases where indirect coupling loss factors (CLFs) must be taken into account have been reported [7,8]. To solve those problems, energy flow method (EFM) computing energy influence coefficients (EIC) between structural subsystems was introduced [9]. This approach allows for more realistic transfer functions by considering indirect couplings which are not negligible in the mid frequency range. In recent studies, the method has been applied for the structural problems to improve accuracy of analysis in the mid frequency range where neither FEA nor SEA is able to provide realistic result predictions. However, this has been limitedly used for vibroacoustic cases to date, whereas its application to the shock response estimation recently demanded in aerospace engineering fields has not been sufficiently investigated.

This paper presents an effective method to be used for shock response estimation in the mid frequency range. In this method, the transfer functions between the excited and the responding subsystem were calculated by EFM unlike the conventional practice that uses transfer functions from SEA. In addition, to incorporate the realistic modal characteristic of the structures in the mid frequency range, shock response spectra of the responding subsystems were extracted by practicing an amplitude correction scheme on the transient time response obtained by input force signal and the reference FRF from FEA [10]. A numerical simulation for a five plate model shows that the proposed method can provide more accurate results than the conventional methods.

2. Theory

2.1. Statistical energy analysis (SEA)

The fundamental SEA power flow relationship can be obtained as a form of the steady state power balance equations when applied to m coupled subsystems as follows [11].

$$\begin{Bmatrix} P_{1,in} \\ P_{2,in} \\ \vdots \\ P_{m,in} \end{Bmatrix} = \omega \begin{bmatrix} \left(\eta_1 + \sum_{i=1,i\neq 1}^{m} \eta_{1i}\right) & -\eta_{21} & \cdots & -\eta_{m1} \\ -\eta_{12} & \left(\eta_2 + \sum_{i=1,i\neq 2}^{m} \eta_{2i}\right) & \cdots & -\eta_{m2} \\ \vdots & \vdots & \ddots & \vdots \\ -\eta_{1m} & -\eta_{2m} & \cdots & \left(\eta_m + \sum_{i=1,i\neq m}^{m} \eta_{mi}\right) \end{bmatrix} \begin{Bmatrix} E_1 \\ E_2 \\ \vdots \\ E_m \end{Bmatrix} \tag{1}$$

where $P_{i,in}$ is the subsystem input power, η_i is the damping loss factor, η_{ij} is the coupling loss factor and E_i is the subsystem energy. The equation can be written as a matrix form

$$\{P_{in}\} = \omega\,[\eta]\,\{E\} \tag{2}$$

Using the SEA power balance equations, the energy response of subsystems can be calculated by inverting the loss factor matrix when the power input vector and loss factor matrix are known or assumed. Other parameters such as average vibration and sound pressure levels can be calculated from subsystem energies. However, there are several hypotheses which determine the validity of this approach. The subsystems must be weakly coupled. Subsystems are said to be weakly coupled if the damping loss factor of each subsystem is much greater than all the coupling loss factors of the subsystem connected with it. Moreover, there must be equipartition of energy in all the modes of a subsystem. This hypothesis is met when the modal overlap factor representing a measure of the overlapping of successive modes in the frequency response function is high, or when the condition of diffuse field is satisfied. In general the above conditions are usually satisfied in the high frequency range. In this case, the high - frequency CLFs are then calculated by computing the transmission coefficient between two semi-infinite subsystems

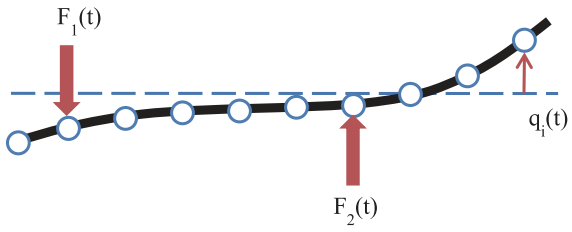

Fig. 1. Discretized, multi-DOF mechanical system.

and averaging over all angles of incidence of the plane. But since it uses only local modes to estimate structural behaviors, application of the SEA approach to the mid-frequency range is limited. Furthermore, the standard FEA method is not applicable either due to large computational load as the degree of freedom of analysis increases dramatically in this frequency region. Therefore, the FE/SEA hybrid method, which maintains the main frame of SEA but incorporates the global mode information from FEA, has been proposed and widely studied up to now [12].

2.2. *Virtual mode synthesis (VMSS)*

The concept of VMSS was first introduced to predict component ballistic shock levels in the combat vehicle design industry and it is currently being applied to aerospace structures [5]. In this approach, it is assumed that the behavior of discretized, muti-degree of freedom (DOF) system subject to external point forces F_1, F_2 as shown by Fig. 1 can be described by the differential equation in a matrix form as

$$\mathbf{M}\{\ddot{\mathbf{q}}\} + \mathbf{D}\{\dot{\mathbf{q}}\} + \mathbf{K}\{\mathbf{q}\} = \{\mathbf{F}(t)\} \tag{3}$$

where $\{\mathbf{q}\}$ and $\{\mathbf{F}(t)\}$ denote n_q – dimensional vector of discretized DOF representing linear displacements and applied forces at specific locations [13]. $\mathbf{M}$, $\mathbf{D}$ and $\mathbf{K}$ are $n_q \times n_q$ mass or inertia, damping and stiffness square matrices respectively. If the mode shape vectors $\{\phi\}_m$ are normalized such that the generalized mass matrix becomes identity matrix, the complex frequency response function (FRF) is obtained as

$$H_{ij}(i\Omega) = \frac{q_i(i\Omega)}{F_j(i\Omega)} = \sum_{m=1}^{n_m} \frac{\phi_{im}\phi_{jm}}{(\omega_m^2 - \Omega^2) + 2\varsigma_m\omega_m\Omega i} \tag{4}$$

where ω_m and ς_m can be expressed by the generalized mass m_m, damping d_m and stiffness k_m as

$$\omega_m = \sqrt{\frac{k_m}{m_m}}, \quad \zeta_m = \frac{d_m}{2\sqrt{k_m m_m}} \tag{5}$$

From Eq. (4), the frequency response of any displacement q_i can be easily determined by adding the contributions for all exciting forces as follows

$$q_i(i\Omega) = \sum_{j=1}^{n_q}\sum_{m=1}^{n_m} \frac{\phi_{im}\phi_{jm}F_j(i\Omega)}{(\omega_m^2 - \Omega^2) + 2\zeta_m\omega_m\Omega i} \tag{6}$$

Virtual modes that allow for mapping to the complex FRF can be allocated in each frequency band based on the modal density of SEA. The result of the virtual mode synthesis process is a vector containing approximations to the mode shape coefficient products for the ith response and jth force at each virtual mode frequency. Under a light damping approximation, the frequency response magnitude becomes a summation of the magnitude of each mode response as

$$|H_{ij}(\Omega)| = \left|\frac{q_i(i\Omega)}{F_j(i\Omega)}\right| = \sum_{m=1}^{n_m} \frac{\phi_{im}\phi_{jm}}{\sqrt{(\omega_m^2 - \Omega^2)^2 + (2\zeta_m\omega_m\Omega)^2}} \tag{7}$$

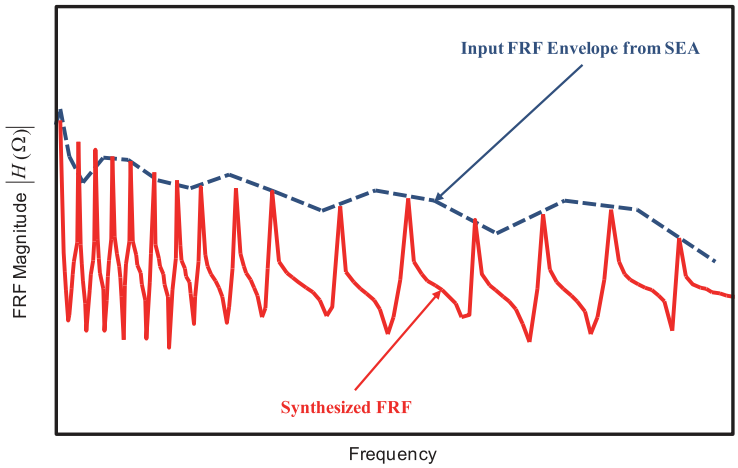

Fig. 2. FRF synthesis by using the FRF envelope from SEA.

and it can be re-written as a product of two vectors

$$|H_{ij}(\Omega)| = \{\Lambda\}^T \{\Phi\}_{ij} \tag{8}$$

where

$$\{\Lambda\} = \begin{Bmatrix} \left[\left(\omega_1^2 - \Omega^2\right)^2 + \left(2\varsigma_1\omega_1\Omega\right)^2\right]^{-1/2} \\ \left[\left(\omega_2^2 - \Omega^2\right)^2 + \left(2\varsigma_2\omega_2\Omega\right)^2\right]^{-1/2} \\ \cdots \\ \left[\left(\omega_{n_m}^2 - \Omega^2\right)^2 + \left(2\varsigma_{n_m}\omega_{n_m}\Omega\right)^2\right]^{-1/2} \end{Bmatrix} \quad \{\Phi\}_{ij} = \begin{Bmatrix} \phi_{i1}\phi_{j1} \\ \phi_{i2}\phi_{j2} \\ \cdots \\ \phi_{in_m}\phi_{jn_m} \end{Bmatrix} \tag{9}$$

The frequency band averaged FRF magnitudes $|H_{ij}(\Omega)|$ required in the VMSS process can be calculated using SEA. As shown in Fig. 2, the FRF including modal information can be synthesized by using the input FRF envelope from SEA and the modal density of the response subsystem, and thus the virtual mode coefficients which are necessary for the transient shock response analysis can be eventually obtained.

2.3. Energy flow method (EFM)

As explained in Section 2.1 SEA is the effective tool for vibro-acoustic analysis for estimating the high frequency behaviors of structures. But it has a limitation in the mid frequency range for the following reasons: In this frequency range, indirect coupling between non connected structures often become dominant. In addition, the CLF has strong dependency on the internal damping of the structure and thus the damping cannot be separated from the coupling loss factors. Therefore the SEA energy balance equation, Eq. (1) which assumes CLFs and damping loss factors (DLFs) as independent variables is no longer valid. To overcome the limitations of SEA, EFM has been proposed. In this method [14], as in SEA, N isolated structures (subsystems) constituting the complete structure are considered and the subsystem total energies $[E]$ and input powers $[P]$ are related by

$$[E] = [A]\,[P] \tag{10}$$

where the $[A]$ is composed of energy influence coefficients (EIC) A_{ij} as follows:

$$\begin{bmatrix} E_1 \\ \vdots \\ E_i \\ \vdots \\ E_n \end{bmatrix} = \begin{bmatrix} A_{11} \ldots A_{1j} \ldots A_{1n} \\ \vdots \ \ddots \ \vdots \ \ddots \ \vdots \\ A_{i1} \ldots A_{ij} \ldots A_{in} \\ \vdots \ \ddots \ \vdots \ \ddots \ \vdots \\ A_{n1} \ldots A_{in} \ldots A_{nn} \end{bmatrix} \begin{bmatrix} P_1 \\ \vdots \\ P_i \\ \vdots \\ P_j \end{bmatrix} \tag{11}$$

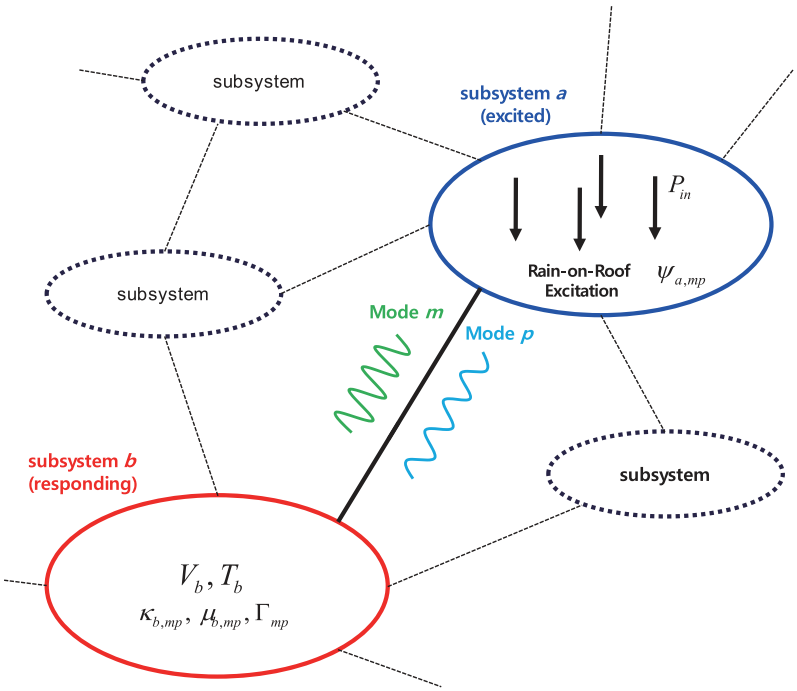

Fig. 3. Nomenclature of EFM model.

By numerically exciting the subsystems one by one, the A_{ij} can be computed:

$$\begin{bmatrix} A_{11} \dots A_{1j} \dots A_{1n} \\ \vdots \ \ddots \ \vdots \ \ddots \ \vdots \\ A_{i1} \dots A_{ij} \dots A_{in} \\ \vdots \ \ddots \ \vdots \ \ddots \ \vdots \\ A_{n1} \dots A_{in} \dots A_{nn} \end{bmatrix} = \begin{bmatrix} \langle E_{11} \rangle & \langle E_{12} \rangle & \dots & \langle E_{1n} \rangle \\ \langle E_{11} \rangle & \langle E_{22} \rangle & \dots & \dots \\ \dots & \dots & \langle E_{kk} \rangle & \dots \\ \langle E_{n1} \rangle & \dots & \dots & \langle E_{nn} \rangle \end{bmatrix} \tag{12}$$

where E_{ij} is the ith subsystem energy for the power input at jth subsystem, and means the spatial averaged values. At high frequencies, the following matrix relation has to be asymptotically satisfied:

$$\begin{bmatrix} A_{11} \dots A_{1j} \dots A_{1n} \\ \vdots \ \ddots \ \vdots \ \ddots \ \vdots \\ A_{i1} \dots A_{ij} \dots A_{in} \\ \vdots \ \ddots \ \vdots \ \ddots \ \vdots \\ A_{n1} \dots A_{in} \dots A_{nn} \end{bmatrix} = \frac{1}{\omega} \begin{bmatrix} \sum \eta_{1i} & -\eta_{21} & \dots & -\eta_{n1} \\ \eta_{12} & \sum \eta_{2i} & \dots & \dots \\ \dots & \dots & \sum \eta_{ki} & \dots \\ -\eta_{1n} & \dots & \dots & \sum \eta_{ni} \end{bmatrix}^{-1} \tag{13}$$

Or in a matrix form:

$$[A] = \frac{1}{\omega} [\eta]^{-1} \tag{14}$$

In EFM, the 'rain on the roof' excitation is usually used to estimate EICs. The 'rain on the roof' loading consists in impulse forces randomly distributed both in time and space over the surfaces of the subsystems defined as

$$F = \sum_{i=-\infty}^{\infty} f_i \, (t - t_i) \delta \, (x - x_i) \tag{15}$$

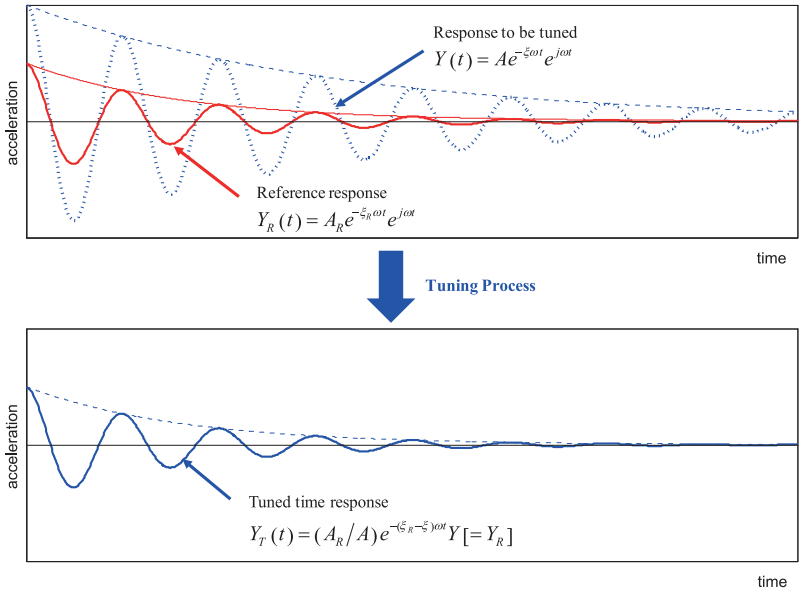

Fig. 4. Tuning of arbitrary shock response time data to reference signal by the amplitude and decay rate ratio.

And the subsystem responses are described in terms of the time and, normally, frequency average kinetic, potential energy in each subsystem. Specifically for the whole system illustrated in Fig. 3, the potential energy V_b, kinetic energy T_b for the responding subsystem b and the power input P_{in} at subsystem a can be determined by a sum of terms involving the interaction of a pair of global modes m, n as follows [9]

$$\begin{aligned} V_b &= \frac{1}{4}\sum_{m,p}\psi_{a,mp}\kappa_{b,mp}\alpha_m^*\alpha_p \\ T_b &= \frac{1}{4}\omega^2\sum_{m,p}\psi_{a,mp}\mu_{b,mp}\alpha_m^*\alpha_p \\ P_{in} &= \frac{1}{2}\mathrm{Re}\left\{i\omega\sum_m \psi_{a,mm}\alpha_m\right\} \end{aligned} \tag{16}$$

where α_m represents the modal receptance, $\psi_{a,mp}$ is the force distribution of the exciting subsystem, $\kappa_{b,mp}$ is the stiffness distribution and $\mu_{b,mp}$ is the mass distribution of the responding subsystem.

In principal, the method has no limitation in application to cases of low modal density and modal overlap, and it can consider indirect coupling CLFs between remote subsystems. Therefore even for the mid-frequency range where both FEA and SEA have their own drawbacks, the method allows for the more accurate estimation of the structural behavior and accordingly the refined transfer functions can be provided by this method for the transient response analysis.

2.4. Time domain correction

The FRFs calculated by the SEA or EFM method have no modal information, so to obtain the time response signals from the complete FRFs, it is necessary to compulsively impose the phase information on them. In the VMSS method, the modes are virtually allocated on the FRF envelopes obtained by the SEA. However, in the current study, to improve accuracy of estimating transient time responses, especially for the mid frequency range, the FRF envelopes were adopted from EFM results. Moreover, the reference FRFs at chosen points obtained by FEA calculations were used to synthesize time responses by time domain correction process. In particular, when the real structure is available, the reference FRF can be obtained without additional efforts.

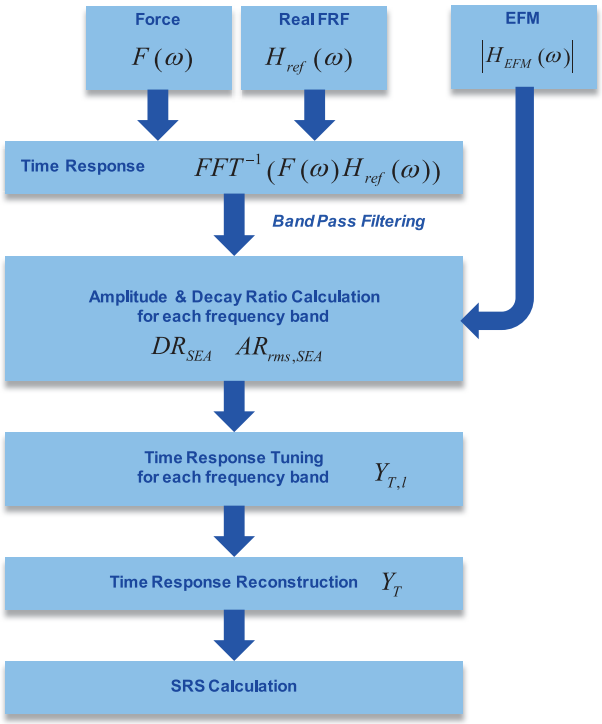

Fig. 5. Time domain correction process.

Generally, time response signals induced by shock excitation are described by the maximum acceleration and decay rate. Thus those values are used to tune a time response signal in reference to another one as illustrated in Fig. 4 [10]

$$\text{Response to be tuned } Y(t) = Ae^{-\xi\omega t}e^{j\omega t} \tag{17a}$$

$$\text{Reference Response } Y_R(t) = A_R e^{-\xi_R\omega t}e^{j\omega t} \tag{17b}$$

$$\text{Tuned Time Response } Y_T(t) = ARe^{-(\xi_R-\xi)\omega t}Y\ [= Y_R] \tag{17c}$$

In Eq. (17), A is the maximum amplitude of acceleration, ξ is the decay rate and AR is the tuning amplitude ratio given by Eq. (18)

$$AR = \frac{A_R}{A} = \frac{Y_{R.rms}}{Y_{rms}}\sqrt{\frac{\xi}{\xi_R}} \tag{18}$$

where $\frac{Y_{R.rms}}{Y_{rms}}$ is referred as the averaged amplitude ratio A_{rms} and $\sqrt{\frac{\xi}{\xi_R}}$ is referred as damping rate ratio DR. These two values are given from the frequency band averaged FRF of the SEA by means of Eqs (19) and (20)

$$AR_{rms,SEA} = \sqrt{\frac{\langle V_{ji}^2\rangle}{\overline{V^2}}} \tag{19}$$

$$DR_{SEA} = \sqrt{\frac{2\xi_{SEA}}{\eta_{j,apparent}}} \tag{20}$$

where $\langle V_{ij}^2\rangle$ means the spatial and frequency band averaged value of the squared velocity on the subsystem j while the subsystem i is excited, and $\overline{V^2}$ and ξ_{SEA} are the band average of the squared velocity and decay rate obtained by

Table 1
Model specifications

Specifications	Values
Material	Aluminum
Dimensions	0.7 m(W) × 1.0 m(H) × 0.002 m(Th)
Mass	3.78 kg/panel
Damping	2.5% (of critical)
Frequency range	up to 1,000 Hz, one third octave
Number of nodes	1836/each panel
Number of elements	1750 quads/each panel
Excitation	Panel #1

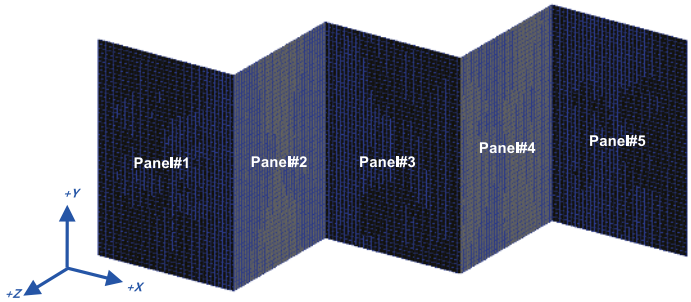

Fig. 6. Five plate model.

the reference FRF, respectively. By applying the tuning process to each frequency band by the above ratios, adding up the band filtered signals and subsequently taking the inverse FFT, the time response signals are synthesized and finally SRSs can be obtained.

$$Y_{T,l} = \left(AR_{rms,SEA}\right)_l \left(DR_{SEA}\right)_l \times BPF_l \left[FFT^{-1}\left(F(\omega)H_{ref}(\omega)\right)\right]$$
$$Y_T = \sum_{l=1}^{L} Y_{T,l} \tag{21}$$

where

l: Frequency band index
$BPF_l[\,]$: the l'th frequency band pass filter
$FFT^{-1}(\,)$: Inverse FFT
$F(\omega)$: FFT spectrum of the excitation force
$H_{ref}(\omega)$: Reference FRF
$Y_{T,l}$: Transient time response of the l'th frequency band
Y_T: Reconstructed transient response

The whole procedure of the time domain correction scheme practiced in this study is summarized in Fig. 5 as a form of flow charts.

3. Analysis and simulation

3.1. Five plate SEA and EFM model

To assess the effectiveness and validity of the proposed method, a five plate model shown in Fig. 6 is considered and the detailed specifications of the model are listed in Table 1. In this model, the five aluminum panels with the same dimensions and material properties are subsequently connected in a zigzag pattern and panel #1 is chosen to be excited. As for the FEA model, to populate more than 10 meshes within a wavelength at the maximum frequency, 1000 Hz, the mesh size is decided by the flexural wave length λ_b or the wave speed c_b as

$$L_{mesh} = \frac{\lambda_b}{10} = \frac{\pi c_b}{5\omega} \cong 0.02 \text{ m} \tag{22}$$

As the first step of the EFM approach, the normal mode analysis is conducted by NASTRAN solver. As a result, a total of 593 eigenfrequencies are extracted up to 1,000 Hz and accordingly the local mass and stiffness matrices of each subsystem which are necessary to obtain the subsystem energy are calculated. Some of the selected mode shapes are illustrated in Fig. 7. From the mode shapes visualized here, it is clear that a certain portion of the vibration energy is transferred by global modes of the plates across the interface lines, thus indirect couplings between remote panels make considerable effects on the structural behavior of the model. In addition, it is shown that as

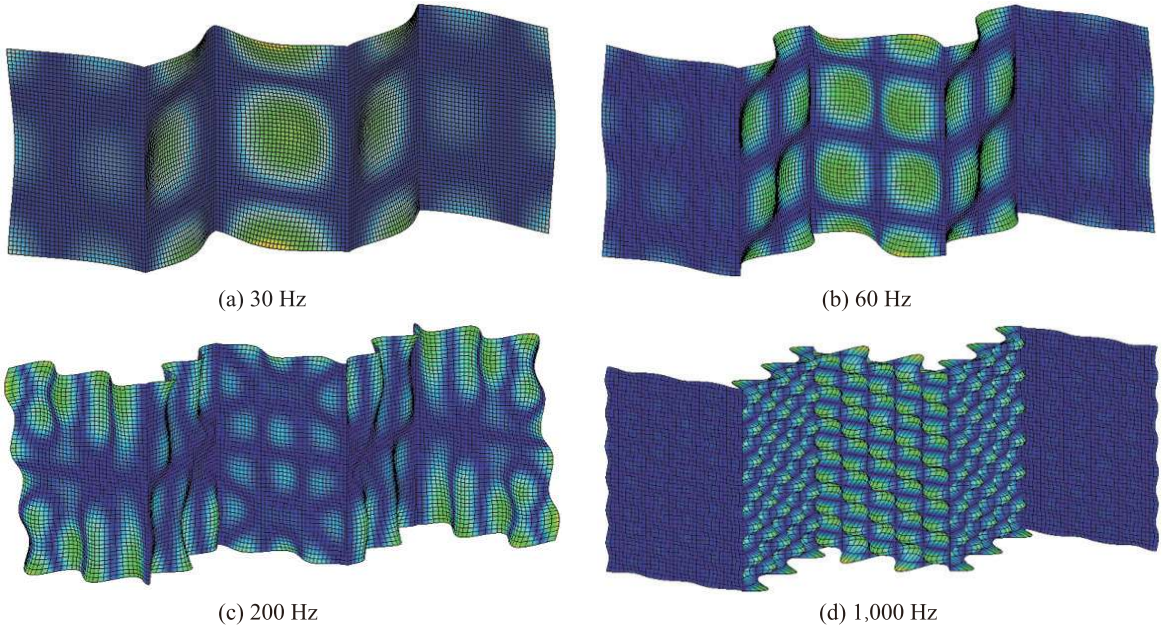

(a) 30 Hz (b) 60 Hz

(c) 200 Hz (d) 1,000 Hz

Fig. 7. Mode shapes of five plate model.

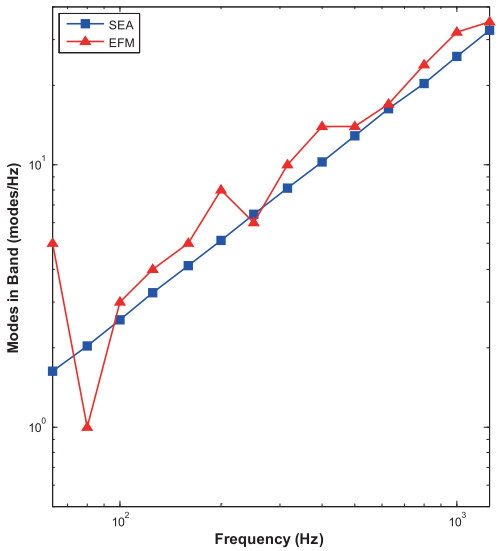

Fig. 8. Modes in band by SEA and EFM.

frequency increases, the modal density also increases and the reverberant field of vibration energy complying with the conditions validating the SEA assumptions appears. In order to verify the advantages of EFM over the standard SEA in the mid frequency range, the primary parameters are calculated by both methods and compared in this range. At first the number of modes has been compared in Fig. 8. In the SEA case, the number of modes in the one third octave band $n(f)$ is given by the area of the plate A, the mass/area m and the flexural rigidity D as follows

$$n(f) = \frac{1}{2} A \sqrt{\frac{m}{D}} \tag{23}$$

By incorporating the modal information adopted by FEA, EFM can represent the realistic distribution of modal energy; even for the structures with geometrical complexity the realistic values can be obtained, while SEA only

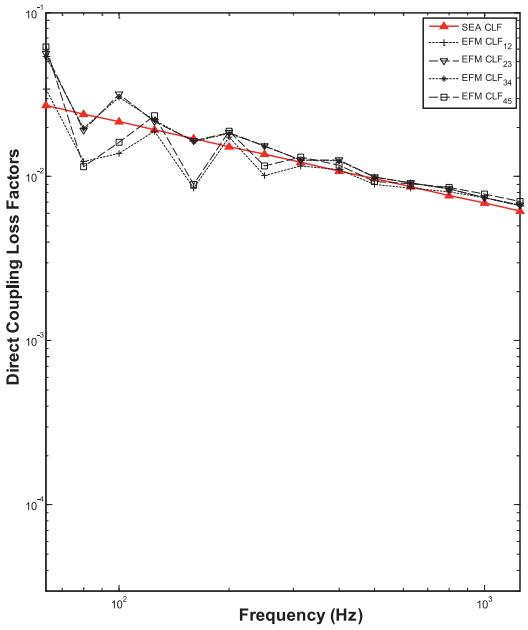

Fig. 9. Direct coupling loss factors by SEA and EFM.

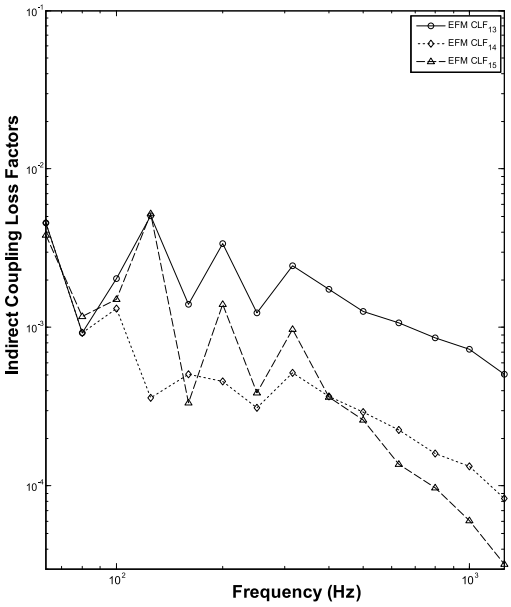

Fig. 10. Indirect coupling loss factors by EFM.

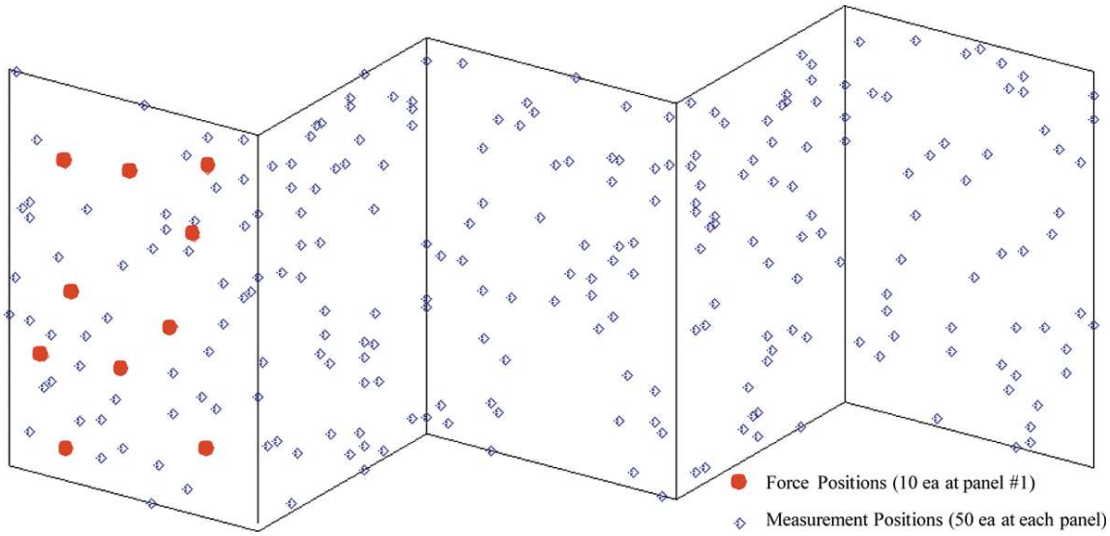

Fig. 11. Numerical simulation model.

gives an approximation. This feature makes EFM suitable for the mid frequency range where the energy of the individual modes becomes quite distinct due to low modal overlap. In this model, simplicity in shape and material properties allows the analytical value by Eq. (23) to estimate the FEA result with good accuracy especially for the high frequency region.

3.2. CLFs and transfer functions

In SEA, CLFs are defined between the physically connected plates assuming their interface line is infinitely long, and incident and radiated waves are plane waves. The plane waves in the plates are processed much like the axial wave fields in beams but the crucial difference is that the waves can make any angle in the range approximately

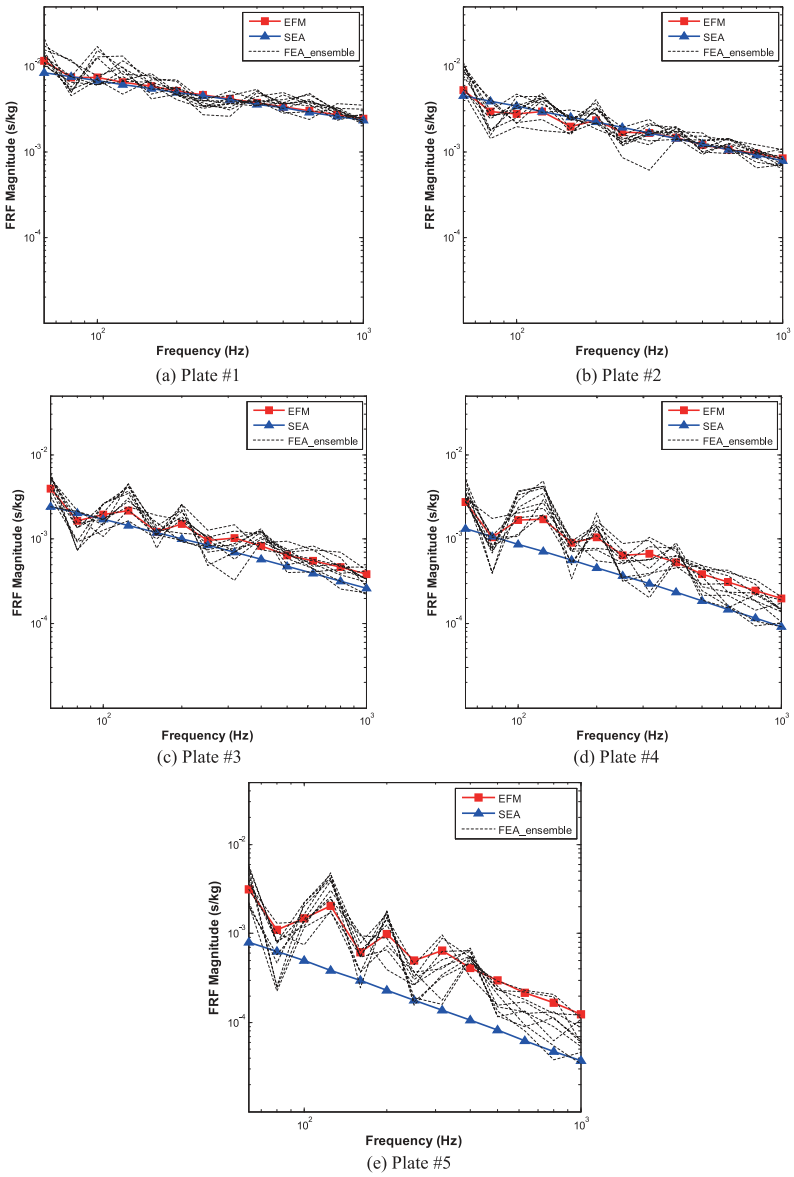

Fig. 12. EFM FRF comparison with SEA and FEA ensemble: For the FEA ensemble, each dotted line represents a spatial average over the FRF magnitudes on the corresponding panel for each force input (a total of 10 inputs on panel #1 are used).

$[0, \pi]$ with respect to the line interface. Thus for the perpendicularly connected plates, the transmission across the interface line is a function of the angle of incidence and the average value of the coupling loss factor over incident angles can be written by

$$\eta_{12} = \frac{c_{g1} L}{\pi \omega A_1} \langle \tau_{12}(\theta) \cos\theta \rangle_\theta \tag{24}$$

where c_{g1} is the group speed in the source subsystem, L is the length of the interface line, A_1 is the area of the source subsystem and $\tau_{12}(\theta)$ is the transmission coefficient at the incident angle θ. Being compared with the standard SEA, in the EFM case, CLFs can be obtained from the off-diagonal entries of the inverse of the EIC matrix and are often called effective coupling loss factors. The term 'effective' is used because the CLFs obtained by inverting the EIC matrix for a single system are deterministic, whereas the CLFs used in SEA are statistical and represent ensemble

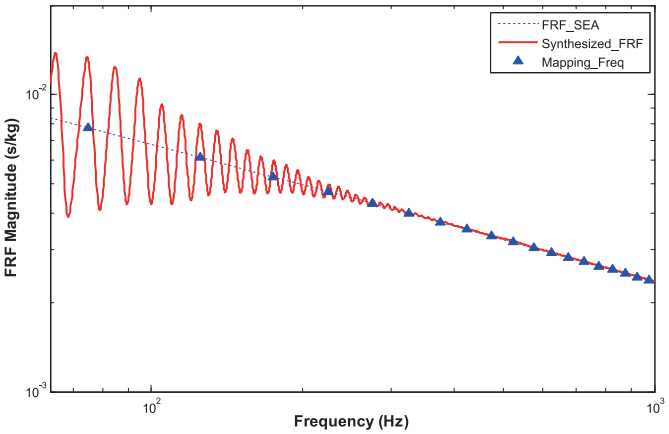

Fig. 13. FRF synthesizing by virtual modes (typical, panel #1).

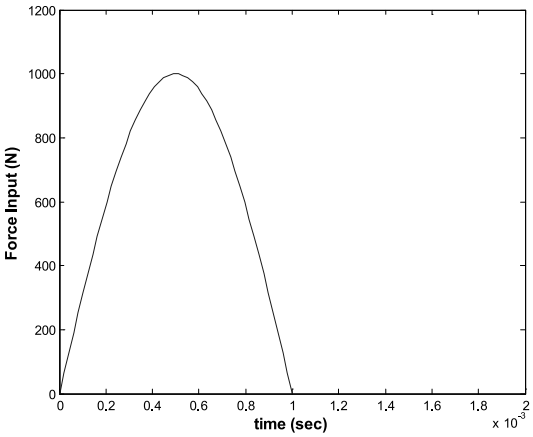

Fig. 14. Half sine input force.

averaged quantities. The effective CLFs between the adjacent panels are calculated by EFM and compared with the analytical values from the standard SEA in Fig. 9. While SEA provides the identical CLFs for all the adjacent panels, EFM yields remarkable differences among the effective CLFs, especially up to 300 Hz, due to global mode patterns. As the frequency increases and accordingly local modes become dominant, the EFM results are asymptotically converged to the analytical value of SEA. For the plates which are not physically connected with the exciting panel (panel #1), EFM provides indirect CLFs as shown in Fig. 10. It is certain that the indirect CLFs tend to decrease as frequency increases but they have a considerable level at low frequencies compared to the direct couplings, therefore they should be taken into account to accurately estimate the structural responses in this range. Particularly, it is noteworthy that up to 400 Hz, the indirect coupling of panel #5 to panel #1 is higher than that of panel #4. This results from the fact that panel #1 and panel #5 have the same orientation and thus they get more easily coupled by means of the global modes.

To investigate the relationship between the force input and the induced responses of the panels, transfer functions were calculated by both SEA and EFM. In addition, to get reference values for comparison with them, the numerical simulation is conducted by FEA direct frequency response analysis with the model as illustrated in Fig. 11. In this simulation, 10 positions for force input on panel #1 and for response calculation 50 positions per each were randomly chosen and the FRFs for these couples of input and response points were calculated and spatially averaged. In Fig. 12, the FRFs by the aforementioned methods are compared for each panel. It is shown that for the panel #1 and #2 that are directly coupled to the input force, the FRFs by SEA and EFM are in good agreement but for the other panels where indirect coupling exists, the EFM result becomes deviated from that of SEA. The deviation appears more significantly for plates #4 and #5. By observing that the FEA numerical simulation results show the same deviations for the remote subsystems, it is confirmed that EFM provides more accurate FRFs in this frequency range, whereas SEA tends to underestimate them by neglecting the indirect couplings. Moreover, from the fluctuated values of FRFs in the low frequency region, it is certain that EFM is capable of representing the uneven modal energy distribution in this region. Consequently, it can be mentioned that EFM has remarkable advantages over SEA for the mid frequency problem by incorporating the realistic modal behavior of structures and thus it can be efficiently used in dealing with transient response problems in this frequency region, especially for parts of structures remote from input sources.

3.3. Standard VMSS

The conventional VMSS using the frequency band averaged FRFs provided by SEA is applied to the five plate model according to the process mentioned in Section 2.2. In order to obtain the force induced responses in SRS of the plates, 5 virtual modes per 50 Hz bandwidth up to 1,000 Hz are allocated and from these virtual mode data the FRFs are synthesized by referencing to the values of the mapping frequencies which are located at the center frequencies of the bands (Fig. 13). At this time, the modal density and the damping for FRF synthesizing are given

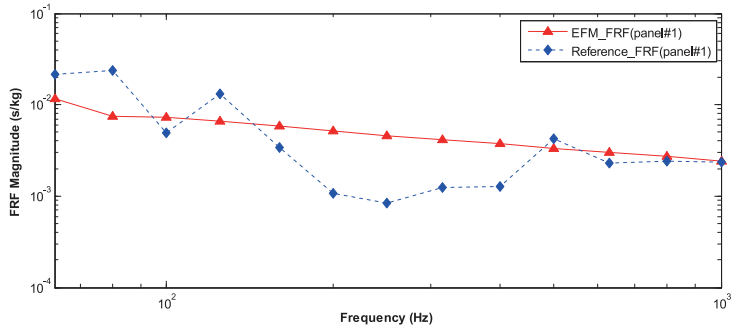

(a) Magnitudes of EFM FRF and Reference FRF (one third octave band, for panel #1)

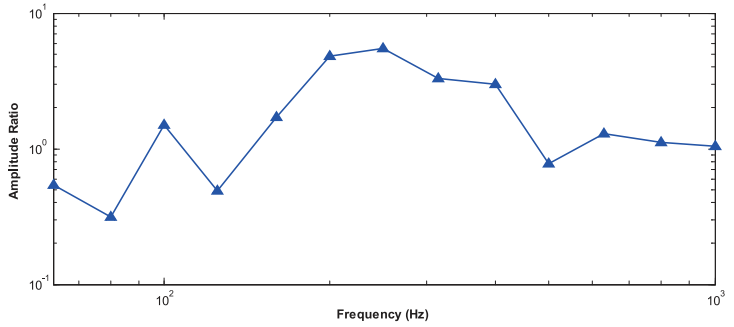

(b) Amplitude Ratio ($|EFM\_FRF|/|ref\_FRF|$)

Fig. 15. Amplitude ratio calculation by EFM FRF and reference FRF (typical, for panel #1).

by the frequency averaged values of the corresponding SEA subsystems and as for the force input, the half sine time signal with a duration of 1 ms and amplitude of 1,000 N simulating a typical pyroshock input is used as shown in Fig. 14.

3.4. Time domain correction with the EFM FRFs

As described in Section 3.2, more accurate FRFs of structures in the mid frequency range can be obtained by practicing EFM. But since these FRFs are frequency averaged values and have no phase information, in order to calculate the shock induced response problems, the complex FRFs have to be synthesized from those data. In this study, the reference FRF at an arbitrary position of the response subsystem is chosen to get a reference FRF and by comparing it with the EFM result, the amplitude ratio is calculated for each frequency band as shown in Fig. 15. The damping rate ratio given by Eq. (20) is assumed to be unity because the same damping values are used for both EFM and FEA calculations. By applying the amplitude ratio to each frequency band of the transient time signal Fig. 16(a) obtained by the input force and the reference FRF as described in Section 2.4, the tuned time response Fig. 16(b) which has the same energy level as EFM response has been obtained. This process is repeatedly applied to each panel to get the SRS responses for all panel subsystems.

3.5. SRS results

Averaged SRS responses for all the panel subsystems are obtained by the proposed method in this study. Figure 17 compares the obtained SRS responses with the response ensemble from direct FEA and the results from the standard VMSS. Because the VMSS results are based on the FRFs from SEA only considering direct couplings, the SRS responses by VMSS decreases along the distance from the force input as in the case of the FRFs from SEA. In particular it is also shown that the VMSS results overestimate the responses of panel #1 and #2 in which only energy transfers through direct couplings exist, whereas they underestimate panels #4 and #5 having indirect couplings with the remote input force. This kind of discrepancy can be easily observed during the shock tests of satellites

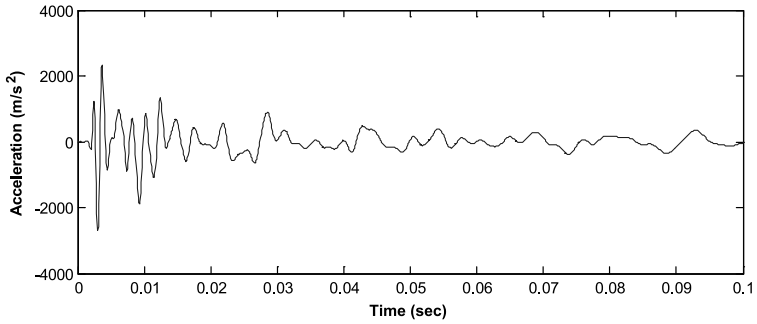

(a) Before time domain correction ($FFT^{-1}\left(F(\omega)H_{ref}(\omega)\right)$)

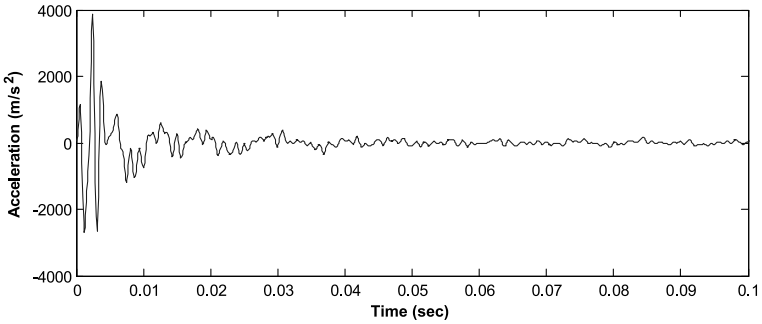

(b) After time domain correction ($\sum_{l=1}^{L}(AR)_l(DR)_l \times BPF_l\left[FFT^{-1}\left(F(\omega)H_{ref}(\omega)\right)\right]$)

Fig. 16. Time signal tuning by amplitude correction factor (typical, panel #1).

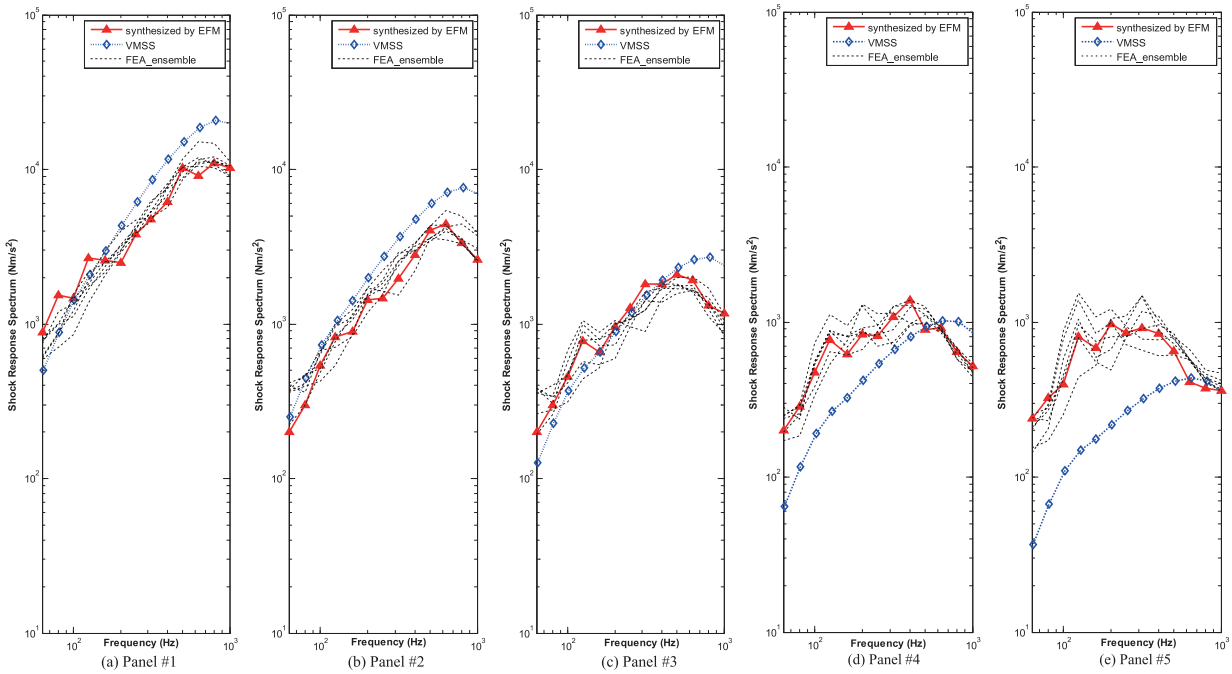

(a) Panel #1 (b) Panel #2 (c) Panel #3 (d) Panel #4 (e) Panel #5

Fig. 17. SRS Comparison of the Synthesized by EFM, VMSS and FEA ensemble: for the FEA ensemble, each dotted line represents a spatial average over the SRS responses on the corresponding panel for each force input (a total of 6 inputs on panel #1 are used).

with structural complexity, particularly for the structural parts that are located farther from the force input position and have strong local modal behaviors [4]. However, the SRSs of the time responses synthesized and tuned by the FRFs from EFM represent good agreement with the FEA calculation. In particular, they show improved accuracy for panels #4 and #5 which are remote from the input subsystem by effectively incorporating the indirect coupling effects and the modal information from FEA. Furthermore, it is noteworthy that the SRS response level of panels #4 and #5 are similar showing small attenuation rate between them, while the others decrease remarkably along the distance from the input force. This is caused by the fact that for those subsystems, the local and modal characteristics of the response subsystems become more dominant than the effects of the propagating wave field transferred from the input force that is fully attenuated up to those points. As proposed in this work, FRFs from EFM are effectively used to estimate the shock responses of structures in the mid frequency range with the current approach.

4. Conclusions

In this study, an effective method to estimate the SRS responses of structures induced by transient force inputs in the mid frequency range is suggested. This method employs the FRFs from EFM, which can accurately represent structural behaviors in this frequency region and a time domain correction scheme, is practiced to obtain the transient time responses from the frequency averaged FRFs. The numerical investigation for a five plate model shows that this approach can provide more realistic shock induced responses for the mid frequency range without having to resort to the large computational load of FEA as long as the reference FRF is available. Practically, this methodology can be applied to cases where the reference FRF is obtainable by direct measurement with the available structure model.

References

[1] C.J. Moening, Pyrotechnic shock flight failures, *Proceedings of the Aerospace Testing Seminar* **8** (1984), 95–109.

[2] Y. Mao, H. Huang and Y. Yan, Numerical techniques for predicting pyroshock responses of aerospace structures, *Advanced Materials Research* Trans Tech Publications, Switzerland, vol. 108–111, 2010, pp. 1043–1048.

[3] A. Girad, E. Courau and L. Bugeat, Pyroshock database for satellites, *Proceedings of the European Conference on Spacecraft Structures, Materials and Mechanical Testing*, (29 Nov 2000).

[4] D.O. Lee, J.H. Han, H.W. Jang, S.H. Woo and K.W. Kim, Shock response prediction of a low altitude earth observation satellite during launch vehicle separation, *Int'l J Aeronautical and Space Sciences* **11**(1) (Mar 2010), 49–57.

[5] E.C. Dalton, A.R.B. Loper, A. Frydman, D. Li and M. Berman, Simulation of ballistic shock in composite armored vehicles, *Proceedings of the 68$^{\text{th}}$ Shock and Vibration Symposium*, Hunt Valley, MD, (Nov 1997).

[6] E.C. Dalton, A. Frydman, D. Li and M. Berman, High frequency shock predictions in armored vehicles: AGS case study, *Proceedings of the 16$^{\text{th}}$ Int'l Symposium on Ballistics* San Francisco, CA, (Sep 1996).

[7] A.M. Wilson, Combined FEA/SEA vibration analysis, *Proceedings of the Fifth International Congress On Sound and Vibration*, (15–18 December 1997).

[8] J.A. Steel and R.J.M. Craik, Statistical energy analysis of structure-borne sound transmission by finite element methods, *Journal of Sound and Vibration* **178**(4) (1994), 553–561.

[9] B.R. Mace and P.J. Shorter, Energy flow models from finite element analysis, *Journal of Sound and Vibration* **233**(3) (2000), 369–389.

[10] I.S. Kim, S.W. Koo and C.G. Hwang, Determination of shock response spectrum using FRF of statistical energy analysis method, *Proceedings of the Korean Society for Noise and Vibration Engineering* **14**(7) (2004), 551–560.

[11] R.H. Lyon and R.G. DeJong, *Theory and Application of Statistical Energy Analysis*, 2^{nd} Edition, Butterworth-Heinemann, Boston, 1995.

[12] M. Buchschmid, G. Müller and A. Kropp, Closing the mid-frequency-gap: Acoustic BIW design using a hybrid sea-fea approach, *Proceedings of the Sixteenth International Congress on Sound and Vibration*, Kraköw, (5–9 July 2009).

[13] AutoSEA-Shock user's guide rev 2, *Vibro-Acoustic Sciences*, 2001.

[14] B. Troclet, B. Hiverniau, M.N. Ichchou, L. Jezequel, K. Kayvantash, T. Bekkour, J.B. Mouillet and A. Gallet, FEM/SEA hybrid method for predicting mid and high frequency structure-borne transmission, *Bentham Open Acoustics Journal* (2009), 45–60.

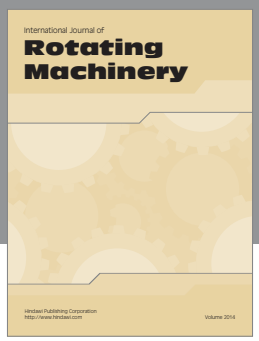

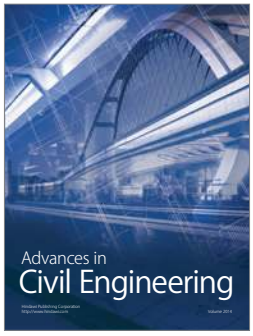

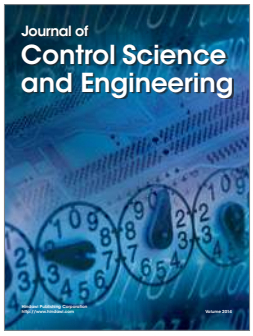

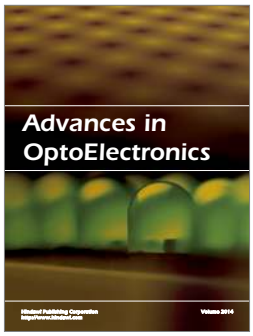

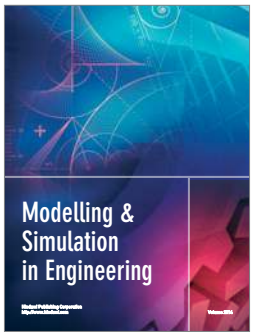

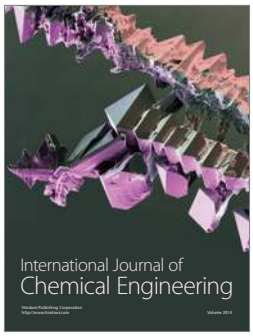

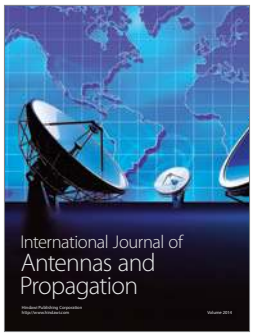

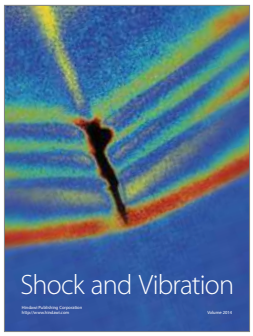

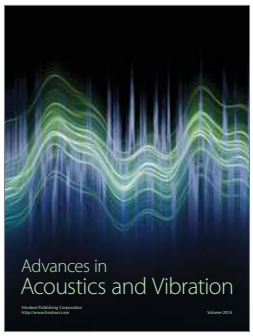

Hindawi

Submit your manuscripts at
http://www.hindawi.com